

5-2013

Molecular Dynamics Simulations of Plastic Deformation in Dopant-Modified Nanocrystalline Metallic Materials

Lucas Brown
University of Arkansas, Fayetteville

Follow this and additional works at: <http://scholarworks.uark.edu/meeguht>

Recommended Citation

Brown, Lucas, "Molecular Dynamics Simulations of Plastic Deformation in Dopant-Modified Nanocrystalline Metallic Materials" (2013). *Mechanical Engineering Undergraduate Honors Theses*. 5.
<http://scholarworks.uark.edu/meeguht/5>

This Thesis is brought to you for free and open access by the Mechanical Engineering at ScholarWorks@UARK. It has been accepted for inclusion in Mechanical Engineering Undergraduate Honors Theses by an authorized administrator of ScholarWorks@UARK. For more information, please contact scholar@uark.edu, ccmiddle@uark.edu.

Molecular Dynamics Simulations of Plastic Deformation in
Dopant-Modified Nanocrystalline Metallic Materials

An Undergraduate Honors College Thesis

in the

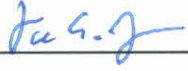
Department of Mechanical Engineering
College of Engineering
University of Arkansas
Fayetteville, AR

by

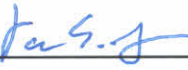
Lucas Matthew Brown

This thesis is approved.

Thesis Advisor:

 DOUGLAS E. SPEAROT

Thesis Committee:

 DOUGLAS E. SPEAROT

 MIN ZOU

Abstract

Polycrystalline metallic materials commonly exhibit the Hall-Petch relationship, which states that decreased grain size leads to increased strength. As a result, nanocrystalline metals, which are defined as polycrystalline metals with average grain diameters on the nanoscale, exhibit ultra-high strength phenomenon. Despite their incredible strength, the applications of these materials are severely limited due to thermodynamic instability that causes low temperature grain growth and a reduction in the enhanced properties. It is known that dopant atoms located at the grain boundaries in nanocrystalline metals can reduce this effect and stabilize the microstructure of these materials, but little is known about the impact they have on dislocation nucleation from the grain boundaries. The goal of this research is to study the effects that antimony atoms segregated to the grain boundaries in nanocrystalline copper have on strength during nanoindentation via molecular dynamics (MD) simulations. In nanocrystalline Cu-Sb alloys, with low concentrations of Sb segregated to the grain boundaries, the microstructure is stabilized, without any significant effect on strength during nanoindentation. In pure nanocrystalline Cu, the location of the indentation has a significant effect on the response of the sample.

Introduction

Nanocrystalline Materials

A crystalline material is a material whose atoms are arranged in a periodic, repeating pattern known as a crystal structure. In a perfect, single crystalline material, the crystal structure will repeat throughout the entire volume of the sample. Polycrystalline materials, such as most metals, are made up of many similarly-sized grains, which are themselves single crystalline with different orientations relative to one

another [1]. The region of atomic misalignment where two grains meet is known as a grain boundary, and it plays a very important role in the strength of materials.

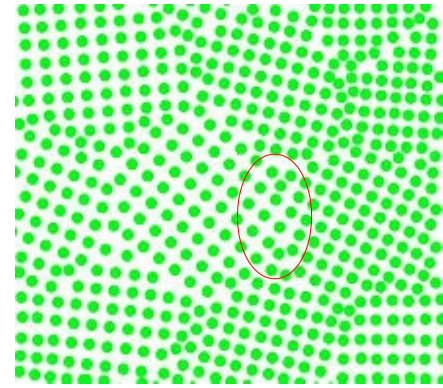


Figure 1: The intersection of two grains is known as a grain boundary [13].

Dislocations are defects in a material; they are deviations from the perfect crystal structure along a line known as the dislocation core [1]. The motion of dislocations through a material plays a huge role

in the strength of a material, causing material failure at much lower stresses than theoretically predicted based on atomic bonding strength. Grain boundaries, then, have a large impact on strength, as they are barriers to dislocation motion and can act as dislocation nucleation sites. In general, the smaller the grains, the more grains are present in a unit volume of material, meaning more grain boundaries and higher strength. This effect is described by the Hall-Petch relationship, and is valid in virtually all metals [2].

$$\sigma_y = \sigma_0 + k * d^{(-1/2)} \quad (1)$$

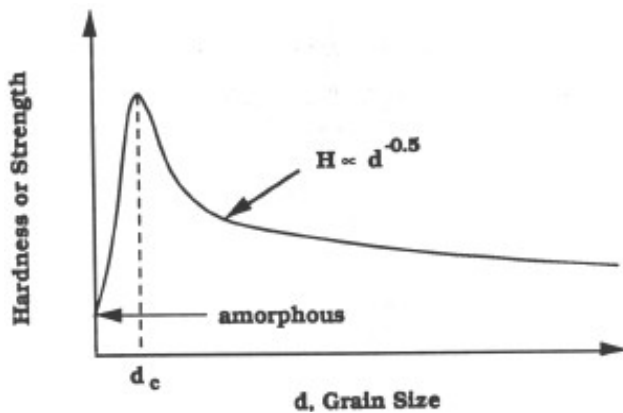


Figure 2: Below a critical grain diameter, the Hall-Petch relation is no longer valid, and strength begins to decrease as grain size decreases [14].

In this equation, the yield strength is represented by σ_y , and the average grain diameter is represented by d ; σ_0 and k are material constants. In an effort to produce increasingly strong materials, average grain diameters have been reduced all the way down to the nanoscale, less than 100nm, creating what are known as nanocrystalline materials. Nanocrystalline materials exhibit what is known as “ultra-strength”

phenomenon; real strengths are approaching ideal strengths closer than ever before [2].

Once grains reach a certain average diameter, usually around 15nm, different deformation mechanisms, such as grain boundary sliding, become more significant, and the Hall-Petch relation is no longer valid. Reduced strength is observed with decreasing grain size; an effect sometimes known as the inverse Hall-Petch relationship [3]. As this effect occurs with grain sizes below 15nm, there is plenty of room for ultra-strength nanocrystalline materials to be created without experiencing the inverse Hall-Petch.

Grain Growth

Although nanocrystalline materials are extremely strong, they experience low-temperature grain growth, severely limiting their use in many engineering applications. In polycrystalline materials, grain growth is experienced at temperatures greater than 50% of their melting temperatures; in nanocrystalline materials, it can occur as low as room temperature [4]. This is a result of thermodynamic instability associated with the fact that there are a lot of grain boundaries, so a lot of atoms are not in their perfect crystal structure alignments [5]. Once grain growth occurs, and the

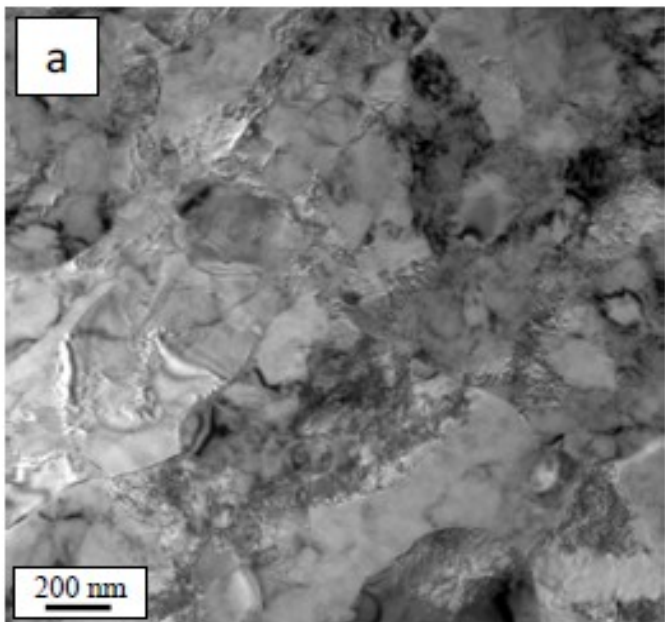


Figure 3a: Before annealing, the nanocrystalline Cu sample has grains on the order of 100nm [5].

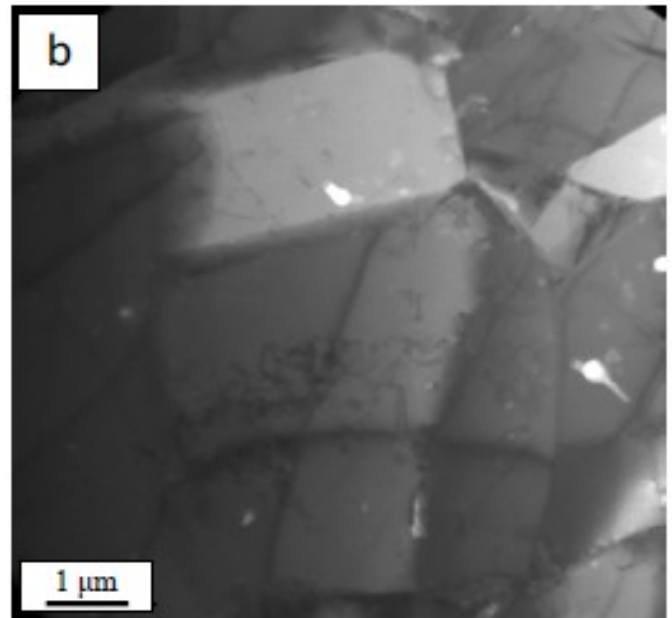


Figure 3b: After annealing, the nanocrystalline Cu sample has grains on the order of 1μm [5].

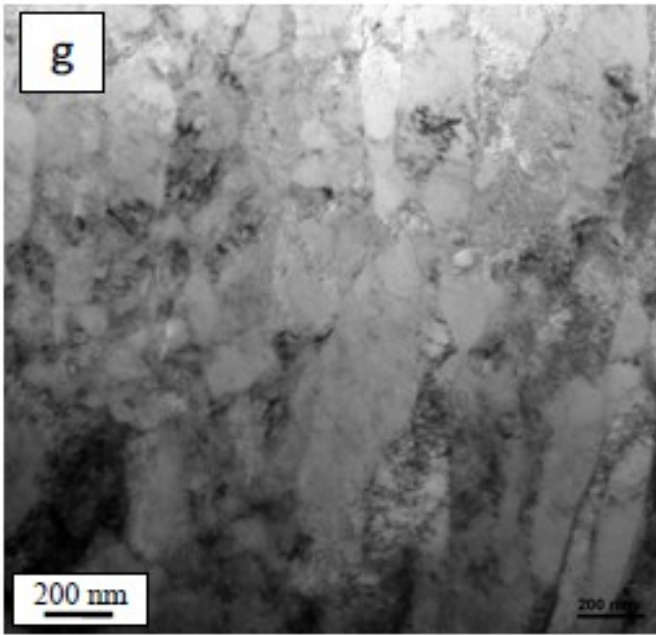


Figure 4a: Before annealing, the grains of this nanocrystalline Cu-Sb sample have diameters below 100nm [5].

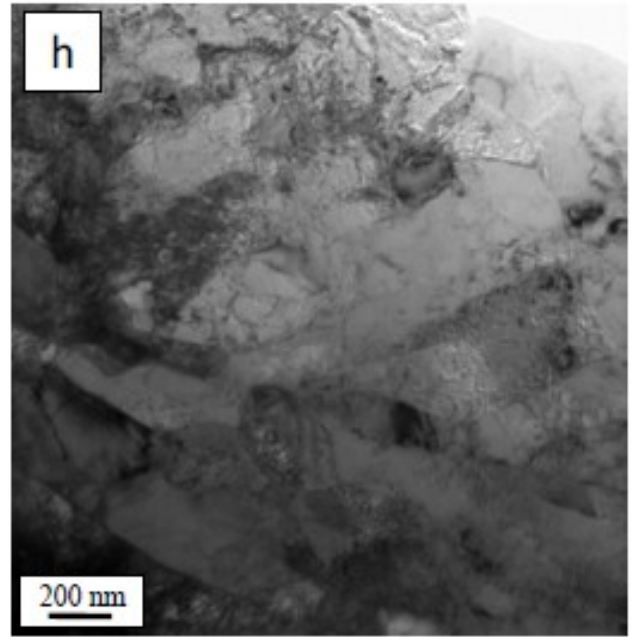


Figure 4b: After annealing, the nanoscale grain size in the Cu-Sb sample as been preserved [5].

nanocrystalline material becomes a coarse-grained material, all of the enhanced properties associated with the nanoscale grain size are lost.

This problem can be remedied. Dopant atoms, which are defined as atoms of a different element intentionally added to a material, located at the grain boundaries in a nanocrystalline material can reduce this low-temperature grain growth effect [5]. *Figure 3* shows a nanocrystalline copper sample before and after a one hour annealing process at 250 °C, a temperature significantly below its melting temperature of about 1100 °C. *Figure 4* shows a similar nanocrystalline copper sample, but with 0.5 atomic percent antimony segregated to the grain boundaries, before and after the same annealing process. The Cu-Sb microstructure is preserved while the pure Cu sample experiences large grain growth. While it is known that dopant atoms can stabilize the microstructure of nanocrystalline metals, little is known about how they impact dislocation nucleation at the grain boundaries.

Objectives

There are three main components of this research: (1) Consolidation and enhancement of code that creates nanocrystalline models for use in molecular dynamics (MD) simulations, (2) Exploration of the effect that the stabilizing antimony dopant atoms segregated to grain boundaries have on the strength of nanocrystalline copper during nanoindentation using MD, and (3) Investigation of the impact of depth, surface area, and position of the indenter on strength during nanoindentation simulations.

Atomistic Simulations and Potentials

Producing pure, fully dense nanocrystalline metallic materials in bulk is difficult, creating an obstacle for researchers wishing to study these materials. However, atomistic simulations have given researchers a way to study difficult-to-produce materials, while providing valuable insight on the atomic scale regarding what is going on during different scenarios, such as plastic and elastic deformation, as well as failure. There are a variety of different atomistic simulation techniques, the one used in this research is called molecular dynamics (MD).

Molecular Dynamics

MD is a computer simulation technique used to model the interactions of atoms or molecules and their interaction with the environment. The simulation works by first determining the forces acting on an atom or molecule at an instant in time, based on a potential function that describes atomic interactions in a specific material or a set of materials. Next, using Newton's second law, or a modified version that accounts for interaction with the environment, the acceleration of the atom or molecule is found. Finally, using the acceleration and a defined time interval, the resulting location of the atom is calculated based on classical mechanics [7]. This process is repeated for every atom or molecule in the

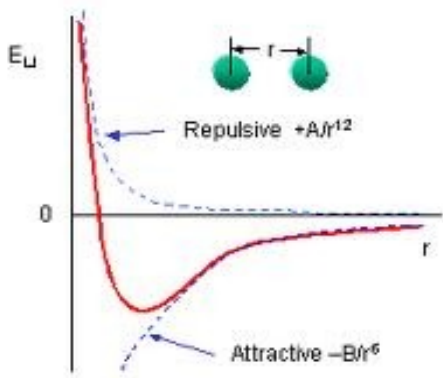


Figure 6: The Lennard-Jones potential is a combination of the repulsive and attractive forces between two atoms [16].

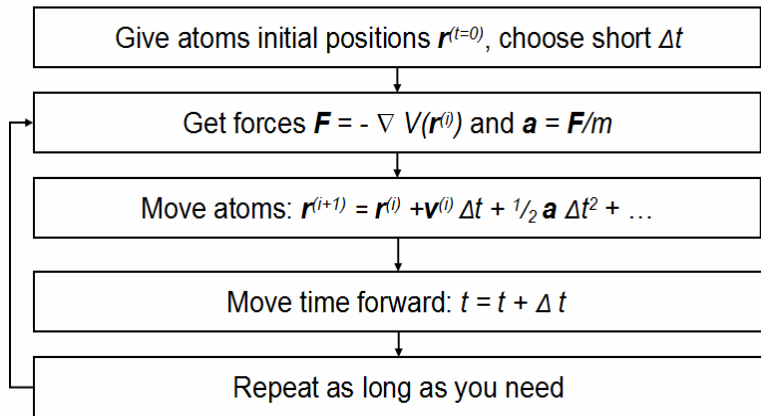


Figure 5: The basic MD algorithm uses Newton's second law to calculate accelerations of atoms [15]. More advanced methods use a modified version to calculate accelerations.

simulation, and then repeated for every time step for the duration of the simulation. MD simulations have already proven extremely useful in the field of materials science [8], and as computational power increases, the simulations will become even more accurate and invaluable.

Interatomic Potentials

The potential function plays a very important role in MD simulations, as it essentially defines how the atoms will react during the simulation [6]. The Lennard-Jones potential is a commonly used potential that uses a combination of repulsive and attractive components, based on the distance between atoms, r . The repulsive component has the form of $1/r^{12}$, with A as a fitting parameter, and the attractive component has the form $1/r^6$, with B as a fitting parameter [9]. The simplicity of this model makes it very appealing from a computational standpoint, but it has limitations with accuracy, partially due to the fact that there are only two fitting parameters.

A more accurate approach for metallic materials is the embedded-atom method (EAM), which takes into account the embedding energy associated with the metallic bonds. EAM potentials define the total

energy of an atom as:

$$E_i = F_\alpha \left(\sum_{j \neq i} \rho_\beta(r_{ij}) \right) + \frac{1}{2} \sum_{j \neq i} \phi_{\alpha\beta}(r_{ij}) \quad (2)$$

In this function, F is the embedded energy as a function of electron density ρ , Φ is a pair potential interaction, and α and β are the elements of the i and j atoms [10].

Voronoi Code Development

The first step in this project is to create the nanocrystalline Cu and Cu-Sb models to be used in the simulations. Wanting to sample grain sizes near the point when the inverse Hall-Petch relation occurs, the average grain diameters of the models selected are 5nm, 10nm, and 15nm. To get a more representative sampling, three different realizations of each are to be built, creating nine models. Additionally, all of these models are then to be doped with varying levels of Sb, located only at the grain boundaries.

Voronoi Tessellations

A mathematical concept known as Voronoi Diagrams or Voronoi Tessellations is used to create nanocrystalline samples. Voronoi Tessellations first appeared in mathematics, and are described by Wolfram Math World as “the partitioning of a plane with n points into convex polygons such that each polygon contains exactly one generating point and every point in a given polygon is closer to its generating point than to any other” [12]. In other words, n random points are created in a plane or volume, then polygons are drawn around each point, such that each point in a polygon is closest to its corresponding point. The idea surfaced in 1644 by Rene Descartes, and later extended to three-

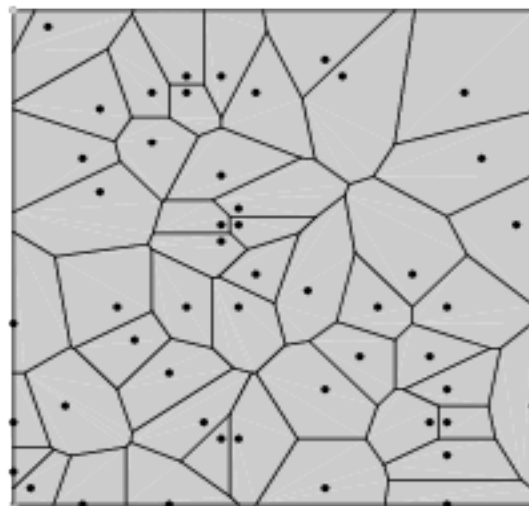
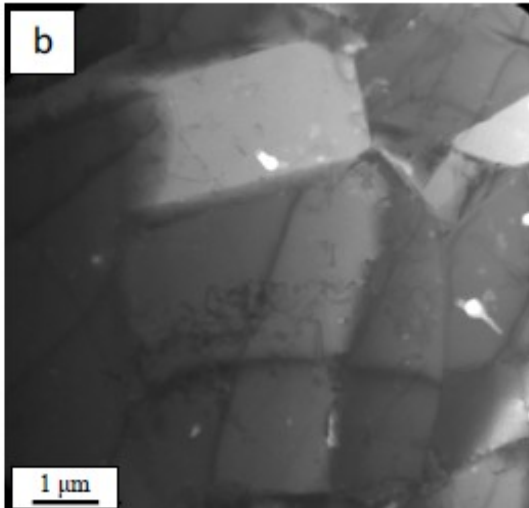


Figure 7: A nanocrystalline Cu sample (top) [5] compared to a Voronoi Tessellation (bottom) [12].

dimensions by Voronoi in 1907 [12]. Figure 7 shows a two-dimensional Voronoi Tessellation diagram and the surface of a real polycrystalline sample; the similarity is remarkable, making the three-dimensional Voronoi Tessellation an ideal candidate for modeling a real nanocrystalline aluminum sample.

The implementation of the Voronoi Tessellation algorithm begins with the user defining the side length of the cubic model to be built, the average grain diameter of the grains in the model, and the lattice parameter of the metal being simulated. Then, the number of grains, n , based on the volume of the simulation cell and an approximation of the volume of the grains are calculated. The grain volume is approximated by assuming the grains are spherical in shape. Next, n randomly generated points, representing

grain centers, are created within the simulation cube. This is the first step of the Voronoi Tessellation algorithm, but to maintain realistic models, a deviation must be taken. In real polycrystalline and nanocrystalline metals, grains are of similar size. To account for this, no two grains are allowed to be created too close to each other, because that would lead to some grains being significantly smaller/larger than the others. If a grain center is created less than a specified distance to another grain center, it is “thrown out,” and a new point randomly generated. Along with coordinates, when each random point is created, a random set of 3 Euler angles are created, which define how the lattice of each grain is rotated relative to the x , y , and z coordinates of the simulation box.

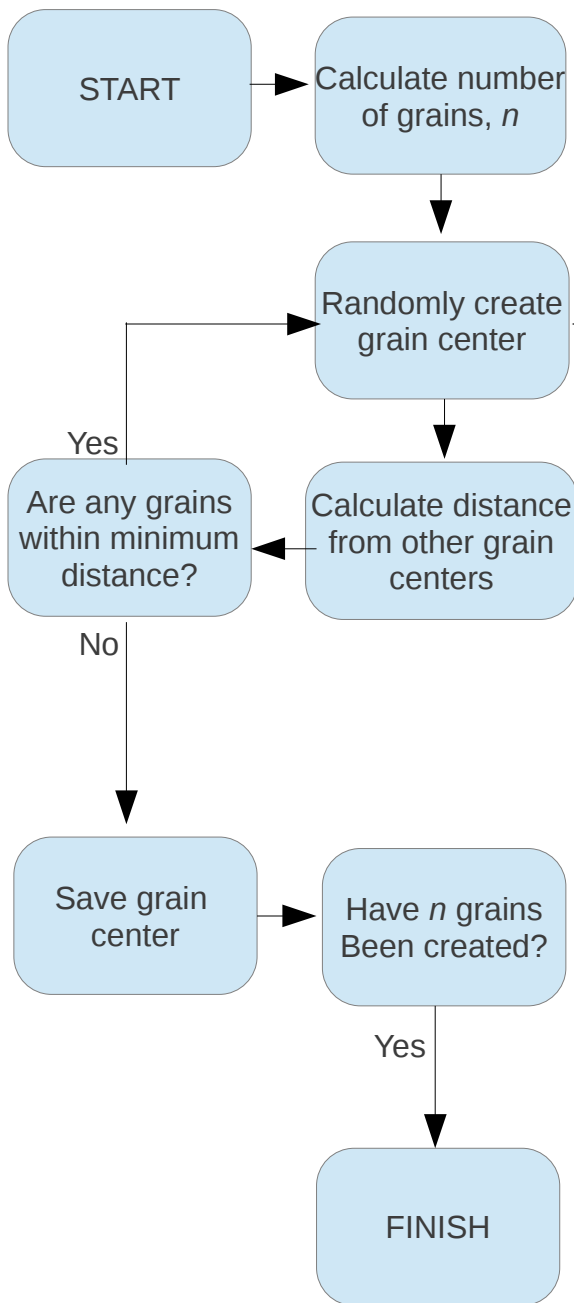


Figure 8: The grain center algorithm used in this work.

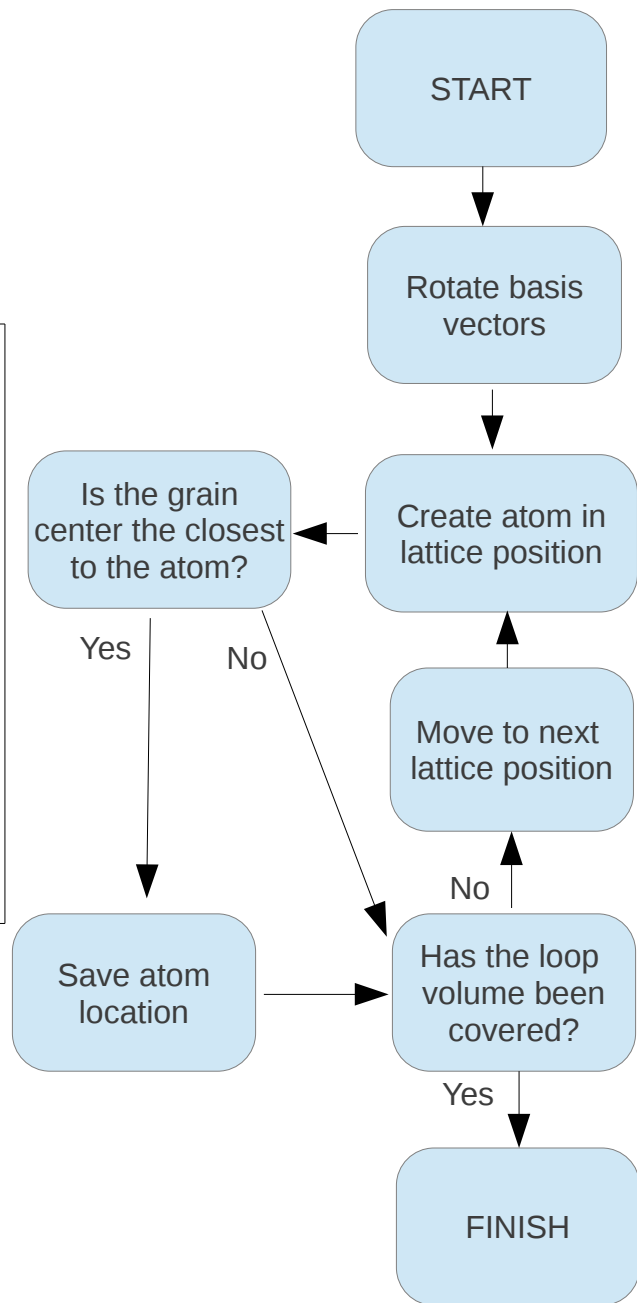


Figure 9: The grain center fill-in algorithm used in this work. This process is completed for each grain center.

Once this process is completed, and all the grain centers and corresponding disorientation angles are determined, atoms were “filled in” following the idea of Voronoi Tessellations. To do this, the program takes a grain center, and creates new basis vectors based on the associated angles, rotating around the standard basis vectors for a given crystal structure (coded for face-centered cubic only at this point).

Once this is done, points are created one at a time, filling a volume covering double the simulation cube side length in every rotated direction. Each time a point is created, its distance from every grain in the sample is calculated; if the current grain center is closest to that atom, it is “kept” and recorded, if not, it is “deleted” and not included as part of the grain. This process repeats for every grain center in the system, completing the model.

Number of Grains

The next step to take in creating the models is to determine how large the model is going to be. There need to be enough grains to produce a statistically relevant representation of a realistic model, in terms of grain size and grain boundary disorientation distributions, but bigger models are computationally more demanding. The goal, then, is to find the smallest model size that would produce a good representative model.

To do this, a cubic model with an average grain

diameter of 5nm that is 10nm on a side is created, resulting in the creation of 15 grains. A histogram of the grain boundary disorientation angles of the grains with respect to the expected Mackenzie distribution are plotted using an Excel spreadsheet built by a former University of Arkansas Ph.D. student, Dr. Rahul Rajgarhia, during his graduate studies. The results are shown in *Figure 10(top)*; it is

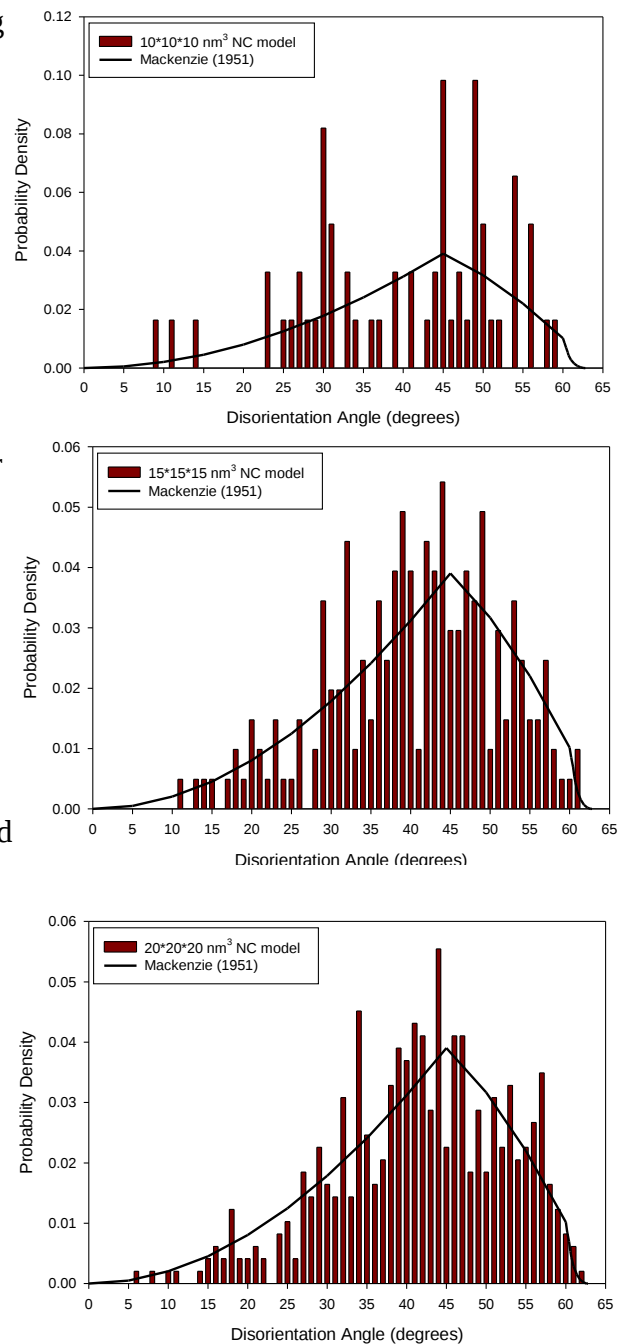


Figure 10: The disorientation of grain boundaries are plotted against the Mackenzie distribution.

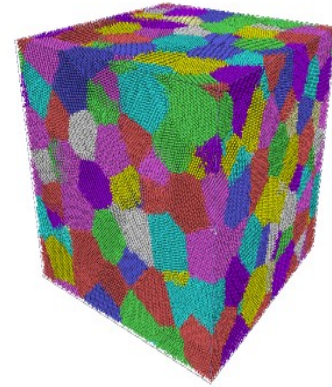
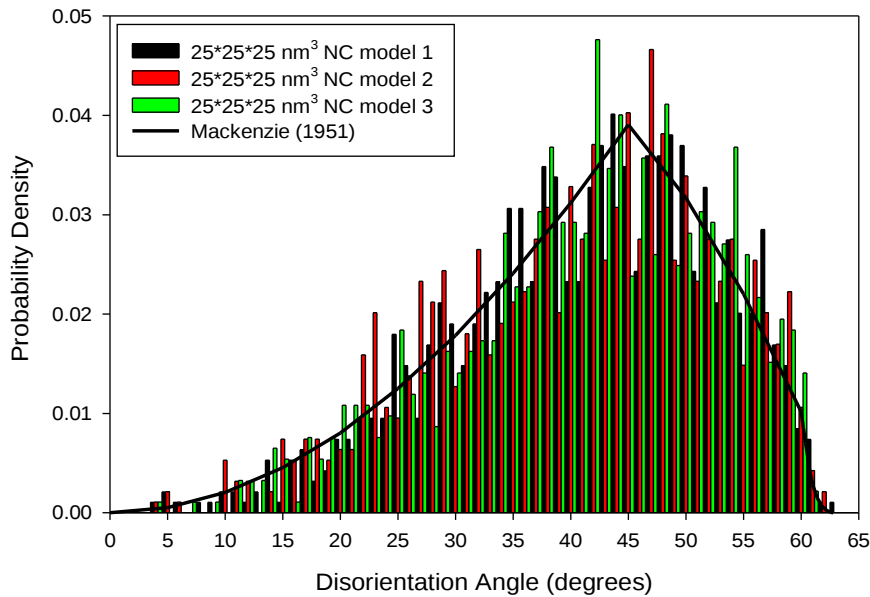


Figure 11: All three realizations of the 240 grain models are plotted against the Mackenzie distribution.

clear that more grains are need. Increasing the side length to 15nm and 20nm yielded models with 52 and 122 grains, respectively, shown in *Figure 10(middle)* and *Figure 10(bottom)* but still far off from the Mackenzie distribution. When increased to 25nm on a side, with 240 grains and 1.32 million atoms, the distribution fit the Mackenzie more closely. Three different realizations of the model are constructed for use in the nanoindentation simulations, and plotted against the Mackenzie distribution as shown in *Figure 11*, along with one of the models.

Scaling the Models

At this point, three different realizations of the 5nm average grain diameter samples are created. The different realizations are created to sample different microstructures. Before building the 10nm and 15nm average grain diameter cases, it was decided that creating different realizations (meaning nine total different realizations between the models) was not efficient. If the effect of dopant atoms changed across different grain diameters, it may not be noticed, being taken as a result of different grain geometry. In order to isolate average grain diameter away from grain geometry, the 5nm grain diameter

models are scaled up to produce the 10nm and 15nm cases.

To accomplish this, part of the process of creating the models was altered. The Voronoi Tessellation method of producing the nanocrystalline models was described in two parts, and it actually requires two different programs to complete. The first part creates the grain centers and the orientation angles, saving this result as a file to be read into another program to fill in the atoms. In order to scale up the 5nm average grain diameter case to the 10nm case, the file containing the grain centers is edited; the side lengths of the cube, as well as the x, y, and z coordinates of every grain center, are doubled. The program used to fill in the atoms is then run taking the edited file as an input, and creating a cube with 5nm sides, 240 grains, and average grain diameter of 10nm, with the same grain geometry as the associated 5nm grain diameter case. This is repeated for the other 10nm grain diameter cases, and for all the 15nm grain diameter cases (with sides and coordinates tripled rather than doubled).

Adding the Sb dopants

With all the pure Cu models built, the final step is to add Sb dopant atoms at the grain boundaries. To do this, grain boundaries are identified based on a parameter called centrosymmetry. Centrosymmetry is a measurement that can be used to determine if a region of a lattice is deviated from the perfect crystal structure, and is given by:

$$CS = \sum_{i=1}^{N/2} |\vec{R}_i + \vec{R}_{i+N/2}|^2 \quad (3)$$

The vectors \mathbf{R}_i and $\mathbf{R}_{i+N/2}$ represent the positions of symmetrically opposite atoms, with respect to the

central atom [11]. In a perfect lattice, the vectors will be equal in magnitude but opposite in direction, so the value will be zero. This calculation is performed using the MD simulator used throughout this research.

Once grain boundary atoms are identified, a program is used to randomly select a number of those to be switched from Cu atoms to Sb based on the desired atomic percent of antimony. The difference between Cu and Sb atoms takes place entirely in the potential function used. As stated previously, atomic interaction are based upon a particular potential function for that material. This potential function is meant for multiple atom types; the user distinguishes which groups of atoms are to be each type of atom. To add the Sb dopants, all those flagged as Sb are labeled as their own group, and that group alone represents Sb atoms in a potential function designed to represent Cu-Sb alloys, with the remaining atoms being Cu. The atomic interactions are modeled using a hybrid interatomic potential; an embedded-atom method (EAM) potential for Cu-Cu interactions and a two-body potential for Cu-Sb and Sb-Sb interactions [6].

Alterations

The Voronoi code is consolidated for easier use and increased speed, and two major functional alterations are made to the original Voronoi code: (1) Any rectangular geometry, rather than cubic only, can be constructed for the simulation cell and (2) The number of grains, rather than simulation box size, can be used as input for creating a model.

Originally, the process required the building of grain centers using Matlab, and filling in the atoms using a Fortran code. The first task is to consolidate this code into one program, allowing the user to start the program and come back later with a finished product instead of having to intervene midway

through, as well as optimizing the code for better performance. Instead of having grain centers and disorientation angles calculated in Matlab, the Fortran code is used to perform that task, store the results globally, then continue on with the construction.

The first functional alteration made is simple; separate x, y, and z box lengths could be input, allowing different geometries to be created instead of restricting to cubic shapes. Next, a second version of the program is made, allowing users to input the number of grains to be in the sample, then have the simulation box size calculated. The program calculates the required volume of the box, based on the number of grains and average grain diameter. Then, based on relative sizes of the side lengths, the simulation box is constructed. Values range from 0 to 1, and relative sizes can be set that way. For example, two sides corresponding to the indentation plane could be set to 1, and the side corresponding to the indentation direction could be set to 0.5, making it half as deep as a cube would be.

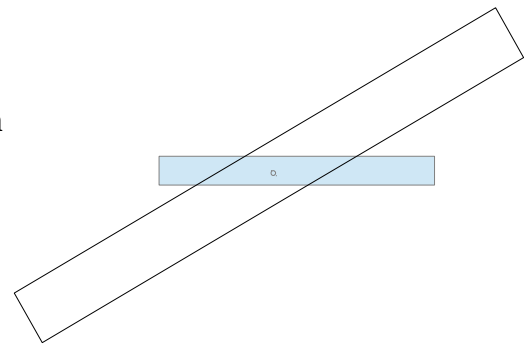


Figure 12: The looping area (outline) does not always cover the simulation area (shaded).

At this point, a critical error surfaced in the code. For thin

samples, where one side is significantly smaller of the others, there are be big holes in the model. After further inspection, the problem persists until the smaller side is around 75% of the other two. The error is due to the fact that the looping parameters that worked well for a cube can not work when one side length is significantly less than the others. Looking at the problem in two dimensions makes it much easier to identify. *Figure 12* shows both the simulation box, and a possible grain center and rotation, outlining the area that would be filled in (double the box in any direction). The points that are not looped over could belong to the grain being created, thus they will not be added to that (or any other) grain in the model. To fix this, the loop volume is adjusted to be that of a cube, with side lengths equal

to double the largest side length of the box. This alteration makes the code slower, but further enhancement by Dr. Spearot significantly increased the speed of the code.

Once working properly, more discrete changes are made to achieve realism. First, the user is able to distinguish periodic and non-periodic directions in the model; previously, all sides were required to be periodic. Second, grains are not permitted to be built within a minimum distance to a non-periodic side. Both of these modifications are made to prevent grains from being unrealistically close to the edge of a sample.

Cu-Sb Nanoindentation

Simulation Parameters

The 5nm average grain diameter samples are indented with an 8nm diameter tip modeled as a strong, spherical repulsive potential. The 10nm and 15nm grain sizes are scaled up to remove grain geometry as a factor to be considered, so in order to insure the same grains were being indented in all three sizes

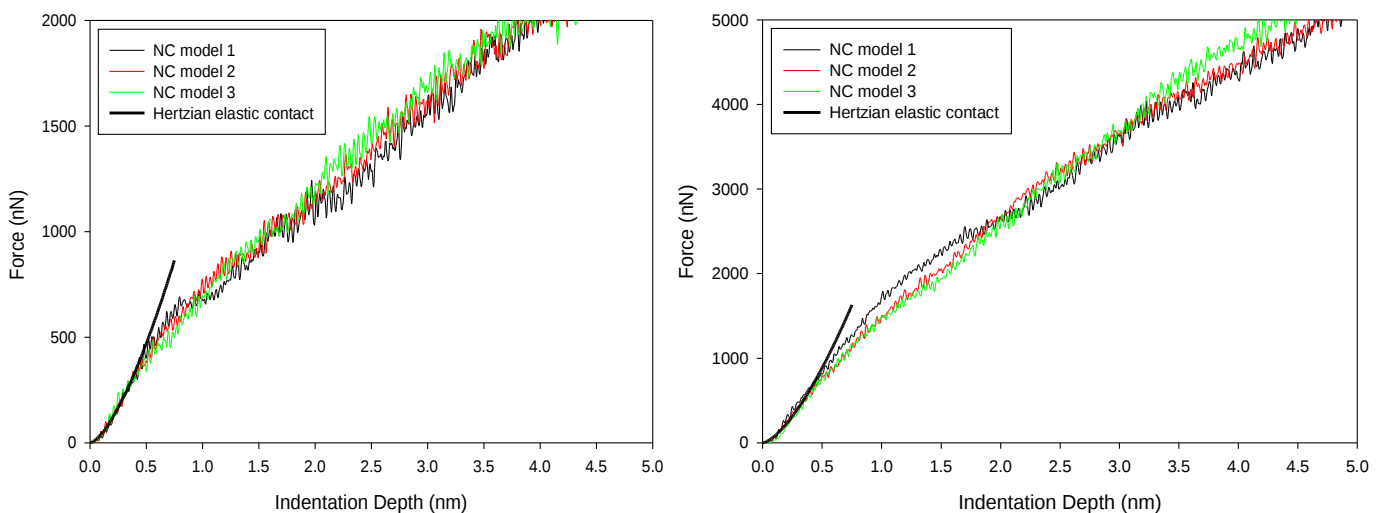


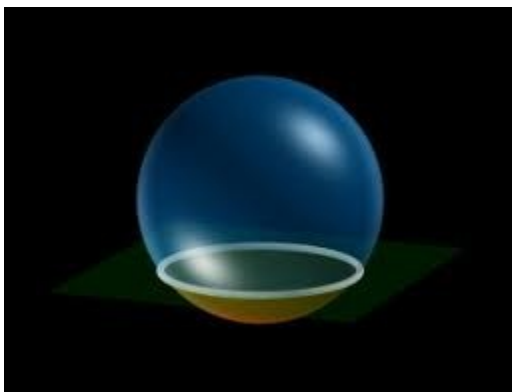
Figure 13: Force-depth curves for pure Cu with 5nm grains (left) and 10nm grains (right) were plotted. The response is elastic and consistent across different microstructures at low indentation depth.

of the same geometry, the indenter is scaled up in the same way the 5nm grain model is; the diameter of the indenter is doubled to 16nm for the 10nm grain diameter models, and tripled to 24nm for the 15nm grains.

To bring the system to equilibrium before indentation, a conjugate gradient method energy minimization is used, followed by an NPT equilibration at 10K for 100,000 steps (or 100ps). The indentation occurs at a 5 m/s displacement rate, and continues for an indentation depth of 5nm. During the nanoindentation, the force that the model exerts on the indenter is recorded for use in analysis.

Results

The first comparison to be made is that of force-depth curves between two different average grain diameter samples. *Figure 13* shows the force-depth curve of the 5nm and 10nm grain diameter models. From these graphs, we can see that the response is elastic and consistent across different microstructures for low indentation depths, followed by deviation from the elastic behavior at larger depths. In addition, the scale of the forces are quite different; the 10nm grain diameter models show



$$r^2 = 2Rd - d^2$$

Figure 14: The indentation area is approximated using the equation (below) [17].

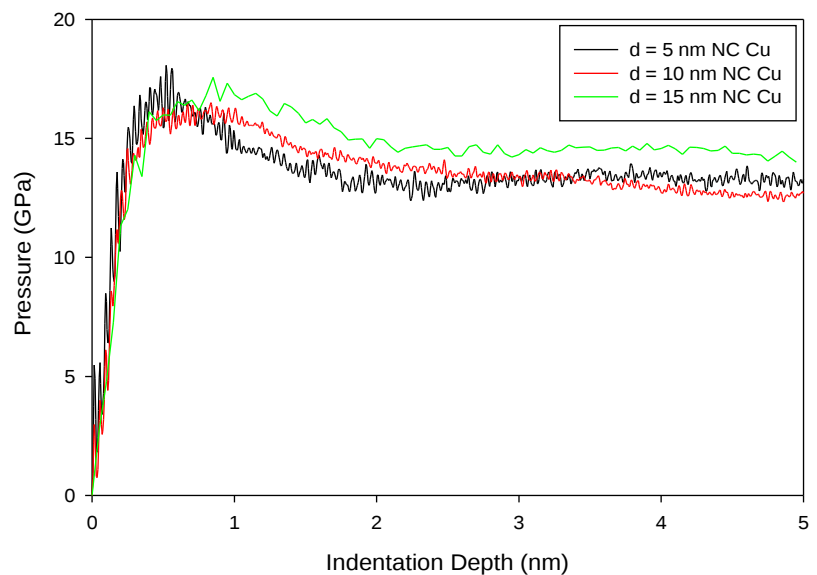


Figure 15: Pressure-depth curves for all three grain diameters of pure Cu show the inverse Hall-Petch effect.

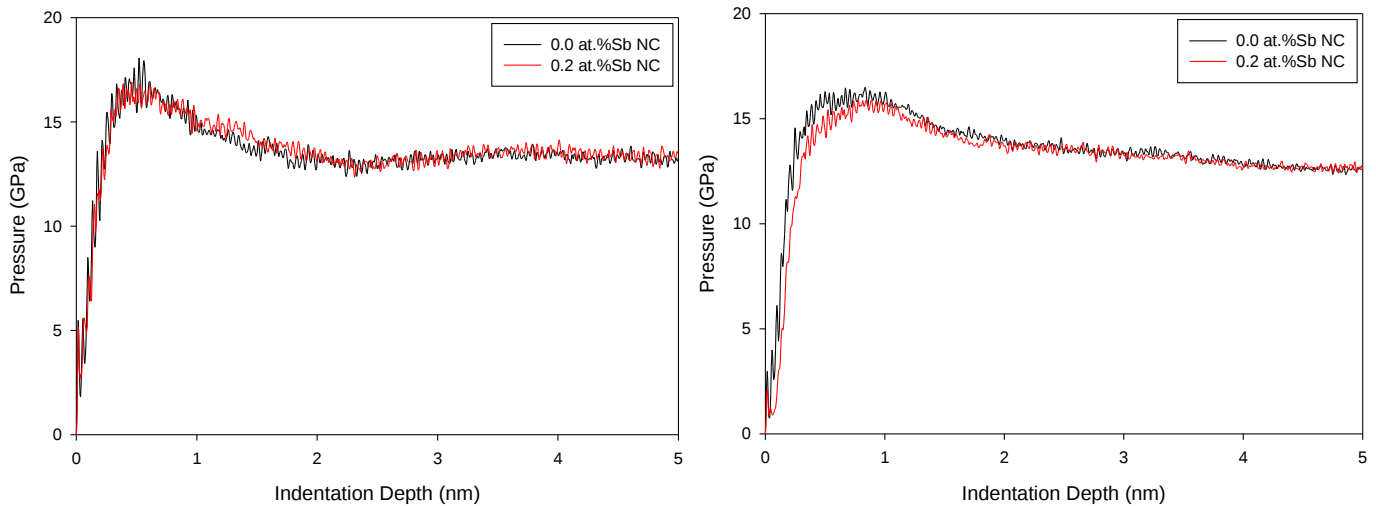


Figure 16: The press-depth curves for pure Cu and Cu-Sb show that the Sb dopant atoms had no noticeable effect on the strength in the 5nm (left) and 10nm (right) grain diameter cases.

much greater force. The forces acting on larger indenters should be larger, because they are coming into contact with significantly more atoms; comparing the force-depth curves to one another is inaccurate, because they represent different size indenters.

In order to adjust the graphs into something comparable, pressure-depth is used instead. The pressure is calculated by approximating the indentation area at each step as a circle represented by the intersection of the top plane of the simulation box and the spherical indenter, as shown in *Figure 14*, along with the equation used for determining the radius of the circle. In the equation, r is the radius of the circle, R is the radius of the indenter, and d is the current indentation depth. The resulting press-depth curves are shown in *Figure 15*; it is clear from these graphs that in decreasing grain diameters from 15nm and below, the inverse Hall-Petch has taken effect, as the pressures decrease with decreasing grain size.

The next observation is the the effect of the Sb atoms located at the grain boundaries in the models. The averages across the three grain geometries of Cu are compared to the those of Cu doped with 0.2 atomic percent Sb in the 5nm and 10nm average grain diameter cases. There is no noticeable

differences between the pure and doped cases at either grain size. Based on these results, in Cu-Sb alloys, where the Sb atoms have segregated to the grain boundaries, the microstructure is stabilized and low-temperature grain growth is reduced, with no noticeable effect on strength, at low atomic percentages of Sb.

Local Geometry in Nanocrystalline Cu

The scaling of the models used in the Cu-Sb work is necessary to isolate the response of the Sb dopants from differences in grain geometry. To evaluate the variance due to grain geometry, a pure nanocrystalline Cu model with 5nm average grain diameter model is selected, and indented in 9

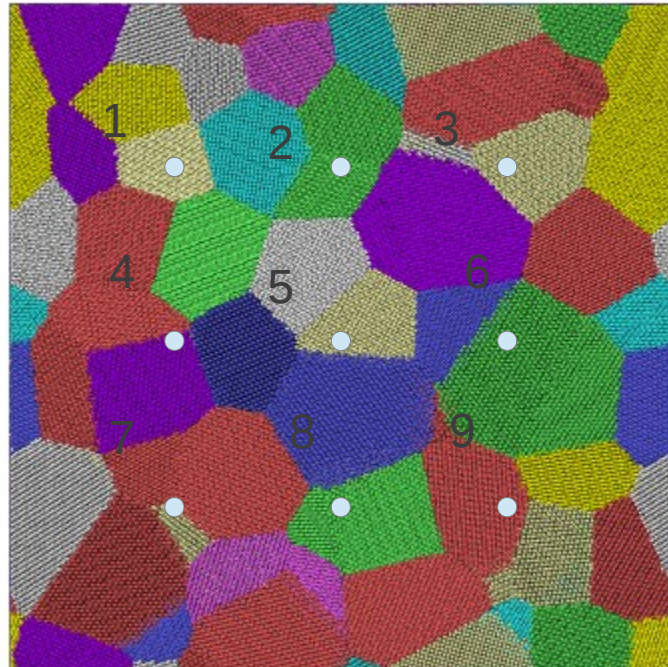


Figure 17: The nanocrystalline model was indented in 9 different, evenly spaced locations.

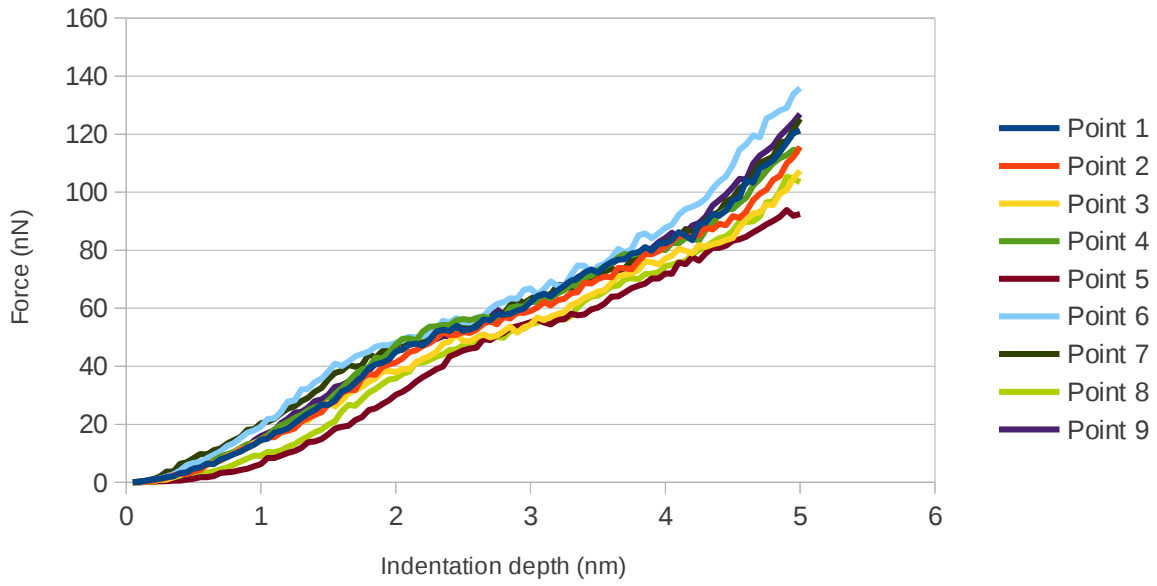


Figure 18: The shape of the force-depth curves of the different indentation locations all have a similar shape.

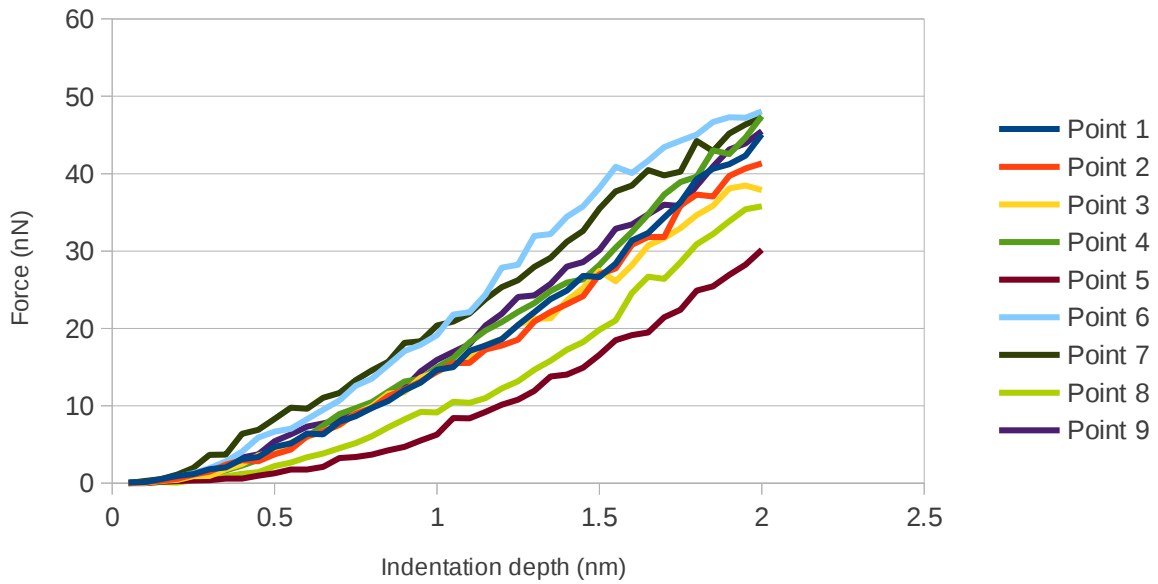


Figure 19: The force-depth curve shows a +/-10nN variance in the forces exerted on the indenter.

different, evenly spaced locations across the indentation surface by a 10nm indenter. Each simulation indents the same sample, but the different locations mean that the geometry in direct contact with the indenter is different in each case. *Figure 17* shows the different locations in the sample used. Note that some indentation points are within a grain, while others are near grain boundaries. *Figure 18* shows the results over the entire simulation. There is little variation on the shape of the force-depth curve between the different locations, but there is $\pm 10\text{nN}$ variation in the force exerted by the Cu sample on the indenter, as shown by plotting the elastic region of the nanoindentation, shown in *Figure 19*.

The force exerted by the Cu is directly related to the pressure on the indenter, leading to the conclusion that the different indentation locations represent differences in strength. Point 7, located directly on grain boundaries, exerts one of the largest forces on the indenter. This correlation is not necessarily true; point 6 exerts a force comparable to that of Point 7, but is located more closely to the center of a grain.

Acknowledgements

All of the simulations for this research were performed using an MD simulator known as LAMMPS (Large-scale Atomic/Molecular Massively Parallel Simulator), developed by Steve Plimpton at Sandia National Labs, and the supercomputing clusters, The Star of Arkansas, Razor Phase 1, and Razor Phase 2, located at the Arkansas High Performance Computer Center at the University of Arkansas. This research was funded in part by a Student Undergraduate Research Fellowship (SURF) grant provided by the State of Arkansas, and by the NSF sponsored Research Experience for Undergraduates (REU) program.

References

- [1] Donald R. Askeland and Pradeep P. Phule. 2006. The science and engineering of materials, fifth edition.
- [2] Ting Zhu and Ju Li. 2010. Ultra-strength materials. *Progress in Materials Science* 55:712-57.
- [3] W. W. Milligan. 2003. Mechanical behavior of bulk nanocrystalline and ultrafine-grain metals. p. 529.
- [4] V.Y. Gertsman and R. Berringer. 1994. On the room temperature grain growth of nanocrystalline copper. *Scripta Metallurgica et Materialia*, 30: 577-81
- [5] Rajgarhia, R. K., Saxena, A., Spearot, D. E., Hartwig, K., More, K. L., Kenik, E. A., & Meyer, H. (2010). Microstructural stability of copper with antimony dopants at grain boundaries: experiments and molecular dynamics simulations. *Journal of Materials Science* 45(24), 6707-6718
- [6] 17. R. Rajgarhia, D.E. Spearot, and A. Saxena: *Comp. Mater. Sci.*, 2008, vol. 44, pp. 1258–64.
- [7] F. Ercolessi A molecular dynamics primer. <http://www.fisica.uniud.it/ercolessi/md/md.pdf> (April 19, 2013)
- [8] S. Jang, Y. Purohit, D.L. Irving, C. Padgett, D. Brenner, R.O. Scattergood. 2008. Influence of Pb segregation on the deformation of nanocrystalline Al: Insights from molecular simulations. *Acta Materialia* 56. 529.
- [9] Lennard-Jones, J.E. (1924), "On the Determination of Molecular Fields", *Proc. R. Soc. Lond. A* 106 (738): 463-477
- [10] LAMMPS user manual. http://lammps.sandia.gov/doc/pair_eam.html (April 19, 2013)
- [11] LAMMPS user manual. http://lammps.sandia.gov/doc/compute_centro_atom.html (April 19, 2013)

[12] <http://mathworld.wolfram.com/VoronoiDiagram.html> (April 19, 2013)

[13] <http://en.wikipedia.org/wiki/File:Crystallite.jpg> (April 19, 2013)

[14] <http://www.msd.anl.gov/groups/im/cmsn/Image1.gif> (April 19, 2013)

[15] <http://en.wikipedia.org/wiki/File:Mdalgorithm.PNG> (April 19, 2013)

[16] <http://employees.csbsju.edu/hjakubowski/classes/ch331/protstructure/ilennardjones2.gif> (April 19, 2013)

[17] <http://archive.msri.org/about/sgp/jim/geom/r4/sphere/sphtor.jpg> (April 19, 2013)